

## Epidote in calc-alkaline magmas: An experimental study of stability, phase relationships, and the role of epidote in magmatic evolution

MAX W. SCHMIDT<sup>1,2</sup> AND ALAN B. THOMPSON<sup>3</sup>

<sup>1</sup>Département Géologie, Université Blaise Pascal, CNRS-URA10, 5 rue Kessler, 63038 Clermont-Ferrand, France

<sup>2</sup>Bayerisches Geoinstitut, Universität Bayreuth, D-95440 Bayreuth, Germany

<sup>3</sup>Institut für Mineralogie and Petrographie, Sonneggstrasse 5, Eidgenössische Technische Hochschule, CH-8092 Zurich, Switzerland

### ABSTRACT

Experiments on tonalite and granodiorite were performed at conditions ranging from 2.1 to 18 kbar and 550 to 850 °C to establish the magmatic stability field of epidote as a function of  $P$ ,  $T$ , and  $f_{O_2}$ .

At water-saturated conditions and  $f_{O_2}$  buffered by NNO, epidote has a wide magmatic stability field in tonalite. At 13 kbar, this field extends from the wet solidus at 630 to 790 °C. The low-pressure intersection of the magmatic epidote crystallization reaction and the H<sub>2</sub>O-saturated tonalite solidus, and hence the minimum pressure for magmatic epidote, occurs at about 5 kbar. The Clapeyron slopes of epidote melting reactions are moderately positive in  $P$ - $T$  space at pressures below the intersection of the epidote melting and the garnet-in reactions at 13 kbar, 790 °C. At this intersection, epidote reaches its maximal thermal stability (790 °C) in tonalite-H<sub>2</sub>O. In the presence of garnet, that is above 14 kbar, epidote melting reactions have steep negative Clapeyron slopes in  $P$ - $T$  space. At  $P$ - $T$  conditions near the low-pressure intersection of the epidote melting reaction with the water-saturated solidus, experiments were also performed with  $f_{O_2}$  buffered by HM. At these oxidizing conditions the magmatic stability field of epidote is enlarged down to a pressure of about 3 kbar. In granodiorite, the stability of epidote has been investigated at pressures from 7.5 to 18 kbar. With respect to the tonalite, the epidote-out reaction is located almost at the same  $P$ - $T$  conditions at 10 kbar, but the maximum thermal stability is about 50 °C lower toward higher pressures. Although few experiments indicate that epidote stability does not increase dramatically with decreasing water activity, at present state it is not possible to predict melting and crystallization behavior of epidote at water-undersaturated conditions. Modal abundances of epidote are low ( $\leq 5$  vol%) in the presence of major (>40 vol%) melt fractions. Thus, epidote in calc-alkaline magmatic rocks is not likely to affect major elements strongly by fractional crystallization.

### INTRODUCTION

Epidote is a common late-stage magmatic mineral in calc-alkaline plutonic complexes of intermediate composition and from relatively deep intrusion level. Its occurrence is a function partly of magma composition and partly of depth of emplacement. Magmatic epidote was recognized as early as 1915 by H.P. Cornelius in the alpine Bregaglia tonalite. Field observations and microscopic textures led Cornelius to conclude "... the only possibility is, that epidote is a primary mineral in our tonalite, crystallizing early from the magma, i.e., before (in part also contemporaneous with) biotite" [translated from German, Cornelius (1915), p. 170, l. 6 ff]. This knowledge disappeared and the petrologic significance of magmatic epidote was ignored until Zen and Hammarstrom (1984) independently recognized epidote as an important magmatic constituent of intermediate calc-alkaline intrusions of the North American Cordillera. These workers also established that epidote appears only in

moderate- to high-pressure intrusions. They estimated a minimum pressure for the crystallization of magmatic epidote between 6 and 8 kbar on the basis of experimental results of Naney (1983) on granodiorite at 2 and 8 kbar. Previously, Crawford and Hollister (1982) estimated a minimum pressure of approximately 6 kbar for magmatic epidote on the basis of the intersection of the curve for epidote stability of Liou (1973) with the melting curve for H<sub>2</sub>O-saturated granite. A low-pressure limit of 6–8 kbar for magmatic epidote was questioned by Moench (1986), who described several epidote-bearing intrusions where pressure estimates from the contact aureoles yielded ~4 kbar.

Several features are considered to be characteristic of a magmatic origin of epidote (Zen and Hammarstrom 1984, 1986; Moench 1986; Tulloch 1986; Zen 1988): (1) A reliable indication is when epidote exhibits strong zonation with allanite-rich cores. However, a lack of such a zonation does not exclude a magmatic origin. (2) An ophitic texture is considered to be typically magmatic. In

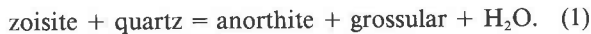
the crystallization sequence epidote seems to appear in tonalites after hornblende but before or contemporaneous with biotite. (3) In calc-alkaline magmatic rocks, the lack of biotite alteration (to chlorite) and a fresh appearance of plagioclase mostly excludes a later retrograde greenschist-facies overprint and therefore makes it unlikely that epidote formed through a subsolidus reaction.

Of course, both primary magmatic and secondary metamorphic epidote might occur together, and an unequivocal identification could be difficult in particular cases. However, for an estimate of intrusion conditions, the presence of magmatic epidote represents a powerful tool. It is easy to identify macroscopically, and its presence excludes a shallow intrusion level for a tonalitic or granodioritic magma.

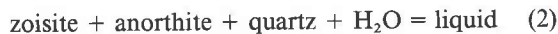
The purpose of this study is (1) to determine experimentally the magmatic stability field of epidote in tonalite and granodiorite at pressures to 15 kbar, (2) to investigate the main factors controlling the occurrence of epidote in calc-alkaline intrusions, and (3) to clarify the role of epidote in magmatic processes.

#### PREVIOUS EXPERIMENTAL WORK RELEVANT TO MAGMATIC EPIDOTE STABILITY

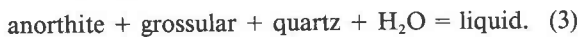
In the most simple system CaO-Al<sub>2</sub>O<sub>3</sub>-SiO<sub>2</sub>-H<sub>2</sub>O (CASH), where epidote-group minerals appear, the subsolidus reaction limiting the stability of zoisite + quartz (Nitsch and Winkler 1965; Newton 1966) is



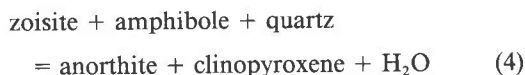
According to Boettcher (1970), near 9 kbar, 775 °C, this reaction intersects the appropriate eutectic H<sub>2</sub>O-saturated solidus reaction, which at lower pressures is



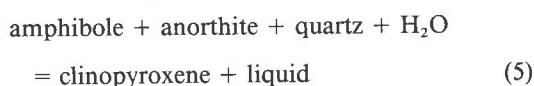
and at higher pressures is



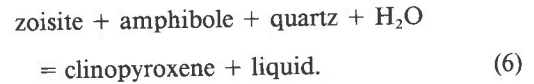
The system CASH, serving also as a model for metamorphism and melting in some calc-alkaline assemblages, apparently generates eutectic melts at quartz- and H<sub>2</sub>O-saturated conditions with compositions between anorthite and zoisite (Boettcher 1970, Reaction 13c). Addition of MgO to CASH provides CMASH (CaO-MgO-Al<sub>2</sub>O<sub>3</sub>-SiO<sub>2</sub>-H<sub>2</sub>O), a model system appropriate to the melting of amphibolite (e.g., Thompson and Ellis 1994). In this system, the subsolidus reaction



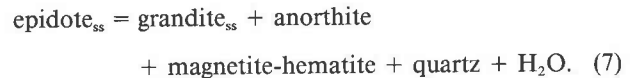
controls zoisite + quartz stability. According to Ellis and Thompson (1986), near 9 kbar, 770 °C, this reaction intersects the appropriate peritectic H<sub>2</sub>O-saturated solidus reactions in CMASH, which at lower pressures is



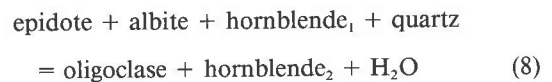
and at higher pressures is



Experiments on Fe-bearing systems at subsolidus temperatures have been performed by Holdaway (1972) and by Liou (1973). Both studies of the synthetic CFASH system at pressures from 2 to 5 kbar showed that the thermal stability of epidote increases with increasing  $f_{\text{O}_2}$ , the breakdown reaction of epidote<sub>ss</sub> (Liou 1973) being



In a natural basalt, Apted and Liou (1983) defined the "high temperature limit of the epidote-amphibolite facies" (from 5 to 7 kbar) through the reaction



where hornblende<sub>2</sub> is richer in Tschermaks-component (Al<sub>2</sub>Mg<sub>-1</sub>Si<sub>-1</sub>) than hornblende<sub>1</sub>.

Experiments by Naney (1983) first demonstrated that epidote is stable above the solidus in granite and granodiorite. At 8 kbar, synthetic granodiorite was found to crystallize epidote up to 700 °C under water-saturated conditions (>12 wt% H<sub>2</sub>O). At water-undersaturated conditions, the epidote-out reaction was lowered by approximately 20 °C. In experiments at 2 kbar, epidote did not occur. Johnston and Wyllie (1988) investigated an Archean trondhjemite at 15 kbar. At water-saturated conditions at 15 kbar, epidote + biotite were observed to be the liquidus phases (approximately 740 °C). At moderately water-undersaturated conditions (>9 wt% H<sub>2</sub>O), epidote remained present to a temperature of 775 °C. Van der Laan and Wyllie (1992) studied the same trondhjemite at 10 kbar, the experiments yielded epidote at 675–700 °C at H<sub>2</sub>O-saturated conditions (>10 wt% H<sub>2</sub>O). Each of these three studies presented phase relationships in isobaric sections with varying temperature and water content. No particular emphasis was placed on epidote stability in these calc-alkaline magmatic rock compositions, and  $f_{\text{O}_2}$  was left to what the experimental apparatus might or might not impose.

As was demonstrated by Holdaway (1972) and Liou (1973) for synthetic systems, by Apted and Liou (1983) for natural basalt in the subsolidus, and, as we shall see, by this study for natural tonalite at temperatures above the water-saturated solidus, the stability of epidote strongly depends on  $f_{\text{O}_2}$ . More oxidizing conditions favor greater temperature and thus lower pressure stability of epidote. In the presence of Fe<sup>3+</sup>, Reaction 1 is displaced to lower pressures because epidote has a higher Fe<sup>3+</sup>/Al ratio than does garnet. This effect was anticipated by Strens (1965) and demonstrated experimentally by Holdaway (1972) and Liou (1973). Thus, although epidote in many intermediate calc-alkaline plutonics is a pressure

indicator, which is to some extent  $f_{O_2}$  dependent, its absence in other intrusions is clearly compositional: Occurrences of magmatic epidote are reported commonly from tonalites and granodiorites but not from more silicic (granites) or more mafic (diorite-gabbros) bulk compositions.

## EXPERIMENTAL CONDITIONS

### Apparatus

The experiments were conducted with the use of different apparatus in three laboratories. Most experiments between 7.5 and 25 kbar were performed in a single-stage piston cylinder with a 22 mm bore at IMP, Eidgenössische Technische Hochschule, Zurich (Table 1). A full salt assembly as described by Schmidt (1992) was used. In this piston cylinder, the applied load pressure was measured directly by a manganin coil and held constant within  $\pm 40$  bars during an experiment by an electronically controlled screw-worm jack. Temperature was measured with a chromel-alumel thermocouple (K-type). Some experiments were conducted in another single-stage piston cylinder with a  $\frac{3}{4}$  in. salt assembly at "Depth of the Earth laboratory," Tempe, Arizona. The assembly was slightly different from the aforementioned in that the upper inner salt cylinder was replaced by crushable alumina. Temperature was measured with WRh thermocouples.

Internally heated pressure vessels with 1 and 2 in. inner diameters equipped with shielded PtRh thermocouples (S type) were used for some experiments conducted at pressures up to 5.2 kbar at Tempe, Arizona. An internally heated pressure vessel with a 7 cm bore was used for some experiments between 5 and 10 kbar at CNRS-URA10, Clermont-Ferrand. There, temperature was measured with PtRh thermocouples (R type). Some low-pressure experiments were conducted at Eidgenössische Technische Hochschule, Zurich, employing conventional René 41 cold-seal pressure vessels pressurized with argon and equipped with an internal thermocouple (K type).

Experimental conditions in the piston-cylinder experiments are considered to be accurate to  $\pm 0.4$  kbar and  $\pm 8$  °C. Experiments in gas pressure vessels were more precise than  $\pm 0.05$  kbar and  $\pm 5$  °C. Gas pressure vessels and piston cylinders at different laboratories were used to allow for the investigation of the pressure range from 2.1 to 18 kbar and because the experiments presented in this study were conducted over a period of several years. Despite the use of different apparatus piston-cylinder experiments were always consistent with each other. In the overlapping pressure range of piston-cylinder and internally heated pressure vessels, consistent results were obtained from all experiments.

For all experiments, a double-capsule technique was used to buffer  $f_{O_2}$  to either nickel + bunsenite (NNO) or hematite + magnetite (HM). Two welded 2.3 mm o.d. Ag<sub>50</sub>Pd<sub>50</sub> capsules containing the sample and 13–15 wt% water were placed together with a 50:50 mixture of nickel and bunsenite, or a 90:10 hematite + magnetite mixture, and approximately 20 mg water into a 4.0 mm o.d. gold

capsule. Sometimes one or three Ag<sub>50</sub>Pd<sub>50</sub> capsules were packed together with the buffer mixture and water into a 4.0 or 5.3 mm o.d. gold capsule, respectively. Experiments were considered as technically successful when water bubbled out of the gold capsule after piercing and when both  $f_{O_2}$  buffer components were present after the experiment. After the experiment silver palladium capsules were analyzed to determine the amount of absorption limit of the microprobe. In all piston-cylinder experiments the initial length of the silver palladium capsules was kept shorter than 5 mm. During the experiments, the distance between thermocouple and the farthest portion of the sample in the double capsule never exceeded 4 mm, which thereby kept the thermal gradient to a minimum. Most experiments lasted between 8 and 15 d (Table 1), but close to the solidus experiment durations of up to 25 d were necessary. When large amounts of melt were present (i.e., at temperatures above 750 °C and at elevated pressures) experiments were as short as 5 d.

### Starting materials

The rocks used were an epidote-bearing tonalite (RPR) from the Alpine Bregaglia intrusion, an epidote-free tonalite (Au164), and an epidote-free granodiorite (Au7) both from the Alpine Adamello intrusion (Table 2). The major constituents of these rocks are amphibole, biotite, plagioclase, quartz, orthoclase (and epidote for RPR); accessory minerals include titanite, magnetite, apatite, and zircon. In some experiments the starting materials were seeded with natural epidote, synthetic almandine, or high Al-hornblende. The natural crystallization pressure of tonalite RPR was approximately 6.5 kbar, and for tonalite Au164 and granodiorite Au7 it was approximately 3 kbar, determined from the Al-in-hornblende barometer (calibration of Schmidt 1992). The samples were ground to a grain size of 10–20  $\mu\text{m}$ . Fifty weight percent of a synthetic glass of identical composition was added to tonalite RPR to enhance reaction rates. The glass was melted from an appropriate mixture of albite, Al<sub>2</sub>O<sub>3</sub>, CaCO<sub>3</sub>, Fe<sub>2</sub>O<sub>3</sub>, K<sub>2</sub>CO<sub>3</sub>, MgO, MnO<sub>2</sub>, SiO<sub>2</sub>, and TiO<sub>2</sub> at 1400 °C and a controlled  $f_{O_2}$  of  $\log f_{O_2} = -6.4$  to obtain an Fe<sup>3+</sup>/Fe<sub>tot</sub> ratio of 0.25 (Kress and Carmichael 1988). For experiments at pressures above 12 kbar the tonalites RPR and Au164 were seeded with 2 wt% synthetic almandine to overcome nucleation problems of garnet. Two weight percent of epidote e04 was added to the granodiorite. This epidote was crushed from an inclusion-free single crystal of almost gemstone quality, kindly supplied by W. Oberholzer from the Geological-Mineralogical Museum, Eidgenössische Technische Hochschule, Zurich. Sample e04 has 0.62 Fe per formula unit (pfu) and contains 0.3 wt% Cr<sub>2</sub>O<sub>3</sub>. This allowed us to distinguish easily e04 seed relicts and newly formed epidote with similar Fe content, the latter always having Cr contents below the microprobe detection limit. Three weight percent of the Al-rich amphibole was added to bracket amphibole compositions.

TABLE 1. Experiment table

Expt.	<i>P</i> (kbar)	<i>T</i> (°C)	<i>t</i> (h)	Seeds	Products	Apparatus
<b>Tonalite (RPR) <math>f_{O_2} = NNO</math></b>						
g11	2.1	850	305		mn-opx, bt, pl, mgt, ilm, liq	ih-a
pe01	3.0	700	576		amp, bt, pl, ksp, qz, liq	cs-z
g01b1	3.8	800	180		amp, bt, pl, liq	ih-a
pe02	4.0	680	624		amp, bt, pl, ksp, qz, mgt, liq	cs-z
g12	5.0	790	304		amp, bt, pl, liq	ih-c
e01	5.2	690	328		amp, bt, pl, qz, liq	ih-a
e02	5.2	730	322		amp, bt, pl, liq	ih-a
r79m	8.5	690	338		amp, epi, bt, pl, liq	ih-c
r79l	8.5	726	338		amp, pl, liq	ih-c
r47	10.0	725	277		amp, epi, pl, liq	pc-z
r72	10.0	750	250	alm	amp, apa, liq	pc-z
r71	10.0	800	232		amp, cpx, liq	pc-z
r34	12.0	550	834	alm	amp, epi, bt, chl, pl, ksp	pc-z
r65	13.0	775	144	alm	amp, epi, liq	pc-a
r80	13.0	795	184	alm	amp, grt, liq	pc-z
r52	14.0	550	860	alm	amp, epi, grt, cpx, chl, phe	pc-z
r68	15.0	800	189	alm	amp, cpx, grt, liq	pc-z
r67	15.0	835	109	alm	amp, cpx, grt, liq	pc-z
r63	16.5	720	136	alm	amp, epi, grt, liq	pc-a
r76	18.0	760	165	alm	amp, epi, grt, liq	pc-z
r78	18.0	790	184	alm	amp, cpx, grt, liq	pc-z
<b>Tonalite (Au164) <math>f_{O_2} = NNO</math></b>						
r55	6.0	665	281		amp, bt, pl, ksp, qz, liq	ih-a
r58	7.5	665	210		amp, bt, pl, ksp, qz, liq	pc-z
r79m	8.5	690	338		amp, epi, bt, pl, liq	ih-c
r79l	8.5	726	338		amp, pl, liq	ih-c
r65	13.0	775	144		amp, epi, liq	pc-z
r80	13.0	795	184		amp, grt, liq	pc-z
<b>Tonalite (RPR) <math>f_{O_2} = HM</math></b>						
ep01	3.0	700	576		amp, bt, pl, ksp, qz, mgt, liq	cs-z
ep02	4.0	680	624		epi, amp, bt, pl, qz, ksp, liq	cs-z
ep06	4.0	770	345		amp, bt, pl, mgt, liq	cs-z
ep08	5.0	670	624		epi, amp, bt, pl, ksp, qz, liq	ih-c
e01	5.2	690	328		epi, amp, bt, pl, qz, liq	ih-a
e02	5.2	730	328		epi, amp, bt, pl, liq	ih-a
<b>Tonalite (Au164) <math>f_{O_2} = HM</math></b>						
ep02	4.0	680	624		epi, amp, bt, pl, qz, ksp, liq	cs-z
ep06	4.0	770	345		amp, bt, pl, mgt, liq	cs-z
e01	5.2	690	328		epi, amp, bt, pl, qz, liq	ih-a
e02	5.2	730	328		epi, amp, bt, pl, liq	ih-a
<b>Granodiorite (Au7) <math>f_{O_2} = NNO</math></b>						
r12	7.5	655	280	epi	epi, amp, bt, pl, qz, apa, liq	pc-z
r79m	8.5	690	338	epi	epi, amp, bt, pl, liq	ih-c
r79l	8.5	726	338	epi	amp, bt, apa, liq	ih-c
r72	10.0	750	250	epi	amp, apa, liq	pc-z
r71	10.0	800	232	epi	amp, apa, liq	pc-z
r13	11.5	655	295		epi, amp, bt, phe, pl, qz, liq	pc-z
r10	13.0	655	655		epi, amp, phe, pl, qz, apa, liq	pc-z
r80	13.0	795	184	epi, alm	amp, grt, liq	pc-z
r55	14.0	750	281	epi	amp, liq	pc-z
r09	15.0	650	381	epi	epi, amp, phe, pl, qz, apa, liq	pc-z
r53	16.5	750	169		epi, amp, grt, liq	pc-z
r76	18.0	760	165	epi, alm	epi, amp, grt, liq	pc-z
r78	18.0	790	184	epi	amp, grt, cpx, liq	pc-z

Note: Abbreviations are as follows: alm = almandine, amp = amphibole, apa = apatite, bt = biotite, cpx = clinopyroxene, epi = epidote, grt = garnet, ksp = potassium feldspar, liq = liquid, mgt = magnetite, qz = quartz, pl = plagioclase, phe = phengite, cs = cold seal pressure vessel, ih = internally heated pressure vessel, pc = piston cylinder, a = at Arizona State University (Tempe), c = at Clermont-Ferrand, z = at Zurich.

### Analytical procedure

The experimental products were examined with a Cameca SX50 microprobe with five crystal spectrometers (ETH) and a Camebax microprobe with three crystal spectrometers (Clermont-Ferrand). Beam conditions were 15 kV, 20 nA and 15 kV, 15 nA, respectively. Data were

processed with PAP- (Pouchon and Pichoir 1984) and ZAF-correction procedures, respectively. Polished longitudinal sections of the capsules were investigated with the use of BSE and SE images to identify the locations of microprobe measurements. Mineral analyses and modal amounts are presented elsewhere.

TABLE 2. Bulk compositions

	Tonalite-andesite				Granodiorite		Trondhjemite
	RPR	Au164	L&W	A&B	Au7	Naney	JvLW
SiO <sub>2</sub>	58.95	59.56	59.14	59.10	66.66	67.15	71.09
TiO <sub>2</sub>	0.71	0.66	0.79	0.94	0.40	—	0.23
Al <sub>2</sub> O <sub>3</sub>	16.80	18.13	18.23	17.80	15.92	17.45	16.15
Fe <sub>2</sub> O <sub>3</sub>	2.36	3.16	2.32	1.78	1.81	2.20	0.33
FeO	3.75	2.55	3.62	4.83	1.65	—	1.05
MnO	0.11	0.12	0.11	0.10	0.11	—	0.03
MgO	3.15	2.63	2.50	3.05	1.58	1.19	0.60
CaO	6.48	6.70	5.92	6.85	4.43	3.52	2.76
Na <sub>2</sub> O	2.83	2.31	3.81	4.27	2.49	3.90	4.93
K <sub>2</sub> O	2.42	1.93	2.19	1.08	2.63	3.99	2.33
P <sub>2</sub> O <sub>5</sub>	0.23	0.20	0.30	0.22	0.12	—	—
H <sub>2</sub> O	1.11	0.94	0.86	0.10	0.79	—	—
Total	98.93	99.00	99.80	100.12	98.66	99.40	100.28
CIPW-norm							
qz	14.8	20.8	11.7	10.1	30.8	20.0	26.0
or	14.6	12.1	13.0	6.4	15.8	23.7	13.2
ab	24.5	19.7	32.5	36.1	21.6	33.3	41.7
an	26.6	32.4	26.5	26.1	21.7	17.5	13.7
cor	—	0.5	—	—	1.2	0.4	0.5
di	3.9	—	1.0	5.2	—	—	—
hy	10.2	7.9	9.5	11.1	5.1	3.0	2.8
mgt	3.5	4.7	3.4	2.6	2.7	—	0.5
hem	—	—	—	—	—	2.2	—
ilm	1.4	1.3	1.5	1.8	0.8	—	0.4
apa	0.5	0.5	0.7	0.5	0.3	—	—

Note: Bulk compositions of Lambert and Wyllie (1974, L&W), Allen and Boettcher (1983, A&B), Naney (1983), Johnston and Wyllie (1988, JvLW), and van der Laan and Wyllie (1992, JvLW) are given for comparison.

### MINERALS, MELTS, AND EQUILIBRIUM

Most experiments were performed at temperatures above the water-saturated solidus where the presence of fluid and melt allowed extensive reaction of the starting material. Phases already present in the starting material (amphibole, plagioclase, biotite, epidote, and garnet) mostly formed idiomorphic growth rims preserving relict cores of initial composition. As expected, the extent to which relict seeds and zonation occurred depended on pressure and temperature, an increase of both favoring reaction progress. Phases that crystallized anew (clinopyroxene, phengite, sometimes also epidote and garnet) formed idiomorphic, almost chemically homogeneous crystals. Generally, the grain size of newly formed crystals was sufficient to obtain microprobe analyses of all experimental products. Specific crystallization features are described below for the experiments with tonalite starting material, if not otherwise mentioned, at  $f_{O_2}$  buffered to NNO. The results presented here do not include the details of experiments close to the solidus (650–655 °C), which are described by Schmidt (1993).

Epidote usually formed small idiomorphic grains (10–15 μm) with rectangular or rhombic shape (Fig. 1). Cores of starting material or compositions intermediate between starting and equilibrium compositions were preserved in most experiments at pressures below 13 kbar, whereas at higher pressures epidote was chemically homogeneous. In some  $P$ - $T$  locations the epidote-out curve was reversed by loading an epidote-bearing (RPR) and

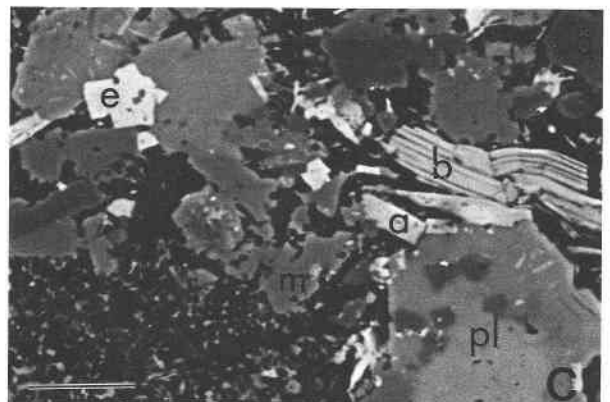
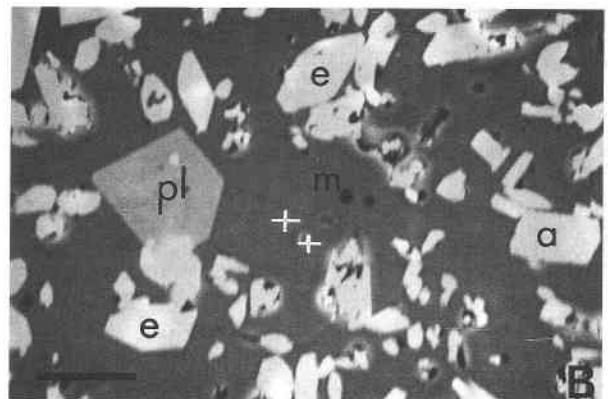
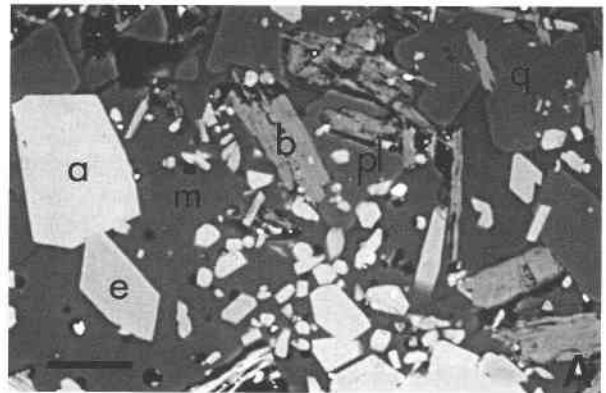
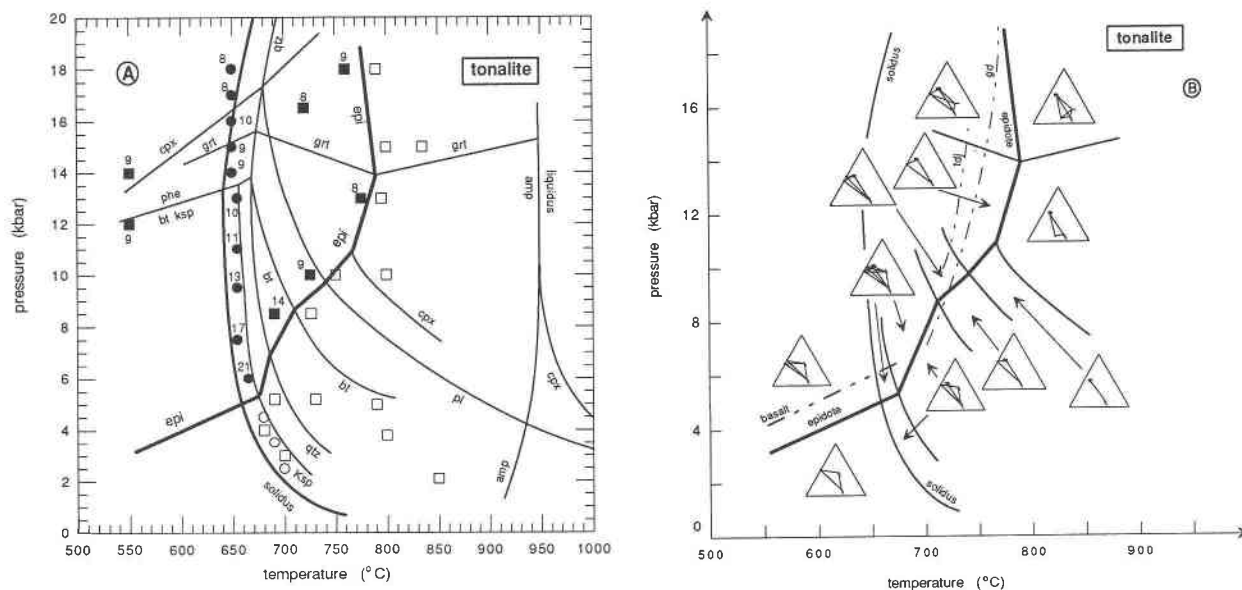


FIGURE 1. BSE images showing magmatic epidote. (A) Close to the solidus, RPR, 6.0 kbar, 665 °C,  $f_{O_2}$  = NNO. (B) Amphibole + epidote + plagioclase + liquid assemblage, RPR, 10 kbar, 725 °C,  $f_{O_2}$  = NNO. (C) Au164, 4 kbar, 680 °C,  $f_{O_2}$  = HM; note that reaction progress in this experiment is poor because of the relatively low pressure and the minor amount of liquid present. Abbreviations are as follows: a = amphibole, b = biotite, e = epidote, m = melt, pl = plagioclase, and q = quartz.



**FIGURE 2.** (A) Pressure-temperature diagram for tonalite melting at water-saturated conditions with  $f_{O_2}$  buffered by NNO. The  $H_2O$ -saturated solidus was determined by Piwinski (1–3 kbar, 1968) and by Lambert and Wyllie (10–20 kbar, 1974) and was slightly modified by Schmidt (1993); the wet liquidus was determined by Egger (0.5–6.3 kbar, 1972) and by Allen and Boettcher (10–16 kbar, 1983). The garnet-in reaction on the liquidus is from Allen and Boettcher (1983). Potassium feldspar is present up to about 20 °C above the solidus in our experiments. The change in slope from the subsolidus to the supersolidus epidote-forming reaction must appear where potassium feldspar disappears and is not directly on the solidus. Assemblages shown as solid symbols contain epidote, and those shown as open symbols do not. Numbers give epidote compositions in

mole-fraction pistacite. Circles are experiments from Schmidt (1993). The disappearance of epidote is represented by reactions with positive  $dP/dT$  until the appearance of garnet near 14 kbar. Biotite instability in tonalite- $H_2O$  continues into a hydration reaction that also involves phengite in the subsolidus region. (B) Schematic representation of the assemblages in tonalite projected into the ACF-de-luxe diagram (Thompson 1982). Because the ACF diagram represents a multidimensional space, crossing tie-lines occur in natural systems (for projection of phases see Fig. 3). Above the quartz-melting reaction, the projection is not strictly valid. The dot-dash lines represent the epidote-out curves in granodiorite (gd = this study), trondhjemite (tdj = compiled from Johnston and Wyllie 1988; van der Laan and Wyllie 1992), and basalt (Apted and Liou 1983).

an epidote-free tonalite (Au164) in the same experiments. No difference in the resulting phase assemblage was observed at pressures above 8 kbar. However, at the low-pressure intersection of the wet tonalite solidus and the epidote-out curve (Fig. 2A), epidote failed to crystallize from tonalite Au164 in two experiments (r55 and r58, Table 1), whereas epidote remained stable and changed composition in tonalite RPR. In experiments with  $f_{O_2}$  buffered to HM, epidote growth was more extensive, and nucleation of epidote in tonalite Au164 was not problematic (Fig. 1C), as both tonalites always yielded identical results. Epidote is relatively Fe-rich at low pressures [ $Ps_{21}$  at 6.5 kbar,  $Ps$  being the molar fraction of the hypothetical end-member pistacite,  $Ca_2Fe_3^{2+}Si_3O_{12}(OH)$ , in a clinzoisite-epidote-pistacite solid solution]; however, Fe contents decrease with pressure to about  $Ps_{10}$  near 10 kbar and to  $Ps_8$  near 18 kbar (at 650 °C) [Table 3, Fig. 2A; for experiments close to the solidus (650–655 °C), see Table 5, Schmidt 1993].

Amphibole formed large prismatic idiomorphic grains up to 40  $\mu m$  in size. Beside the large crystals, which com-

monly preserved cores with starting-material composition, long fine-grained prismatic amphiboles (<15  $\mu m$ ) nucleated (Fig. 1B). The latter were chemically homogeneous. Amphibole composition was bracketed in some experiments by using seeds of different composition in the starting material. Amphiboles were mostly hornblende and tschermakite (Table 3). At temperatures above 780 °C and pressures  $\geq 10$  kbar very small amounts of small augitic clinopyroxene (usually <10  $\mu m$ ) formed from the melt. With increasing pressure jadeite contents increased slightly, and clinopyroxenes grew larger, forming crystals up to 50  $\mu m$  in size. The minor amounts of augitic clinopyroxene did not reveal a significant influence on the crystallization behavior of amphibole.

Biotite occurred mostly in experiments  $\leq 8.5$  kbar and was present as long tiny flakes, typically  $25 \times 5 \mu m$  in size. Plagioclase formed wide (5–20  $\mu m$ ) idiomorphic growth rims often upon preserved cores of starting-material composition (Figs. 1B and 1C). At pressures just above the garnet-in reaction (Fig. 2A) and temperatures below 750 °C, garnet formed thin (maximum 5  $\mu m$ ) growth

TABLE 3. Phase analyses of selected experiments

Expt. P (kbar) T (°C)	r47				r65			r76			
	epi	amph	plag	melt	epi	amph	melt	epi	amph	gar	melt
SiO <sub>2</sub>	39.03	42.17	56.44	60.12	38.72	43.75	59.60	39.26	44.96	38.32	64.70
TiO <sub>2</sub>	0.77	1.19	0.04	0.19	0.39	0.74	0.09	0.45	0.45	0.58	0.12
Al <sub>2</sub> O <sub>3</sub>	29.76	17.43	27.07	14.69	30.05	15.00	15.55	30.49	15.40	21.41	14.19
Fe <sub>2</sub> O <sub>3</sub>	4.64	3.06	0.46	—	4.18	2.17	—	4.64	2.74	0.00	—
FeO	—	11.01	—	1.51	—	10.99	1.32	—	9.85	23.31	0.74
MnO	0.26	0.27	0.00	0.01	0.04	0.08	0.03	0.07	0.04	0.33	0.01
MgO	0.68	9.54	0.00	0.34	0.36	10.71	0.26	0.57	11.42	5.04	0.35
CaO	21.95	10.28	8.92	4.13	23.27	11.09	3.96	22.75	9.91	9.89	2.43
Na <sub>2</sub> O	0.02	1.78	6.40	2.48	0.08	1.99	3.13	0.02	2.21	0.05	2.55
K <sub>2</sub> O	0.08	0.81	0.22	2.22	0.06	0.90	1.87	0.05	0.95	0.06	2.76
H <sub>2</sub> O	1.95	2.05	—	n.d.	1.94	2.05	n.d.	1.96	2.08	—	n.d.
Total	99.14	99.59	99.58	85.71	99.12	99.49	85.81	100.27	100.02	99.00	87.84
Si	3.012	6.166	2.542	3.073	2.997	6.400	3.041	2.998	6.480	2.999	3.182
Ti	0.045	0.131	0.001	0.008	0.023	0.082	0.004	0.026	0.049	0.034	0.004
Al	2.707	3.004	1.437	0.885	2.741	2.588	0.935	2.744	2.617	1.976	0.823
Fe <sup>3+</sup>	0.269	0.337	0.016	—	0.244	0.001	—	0.266	0.297	—	—
Fe <sup>2+</sup>	—	1.347	—	0.065	—	0.239	0.056	—	1.188	1.526	0.031
Mn	0.015	0.034	0.000	0.001	0.002	1.345	0.001	0.004	0.005	0.022	0.000
Mg	0.078	2.078	0.000	0.026	0.042	0.010	0.020	0.065	2.454	0.588	0.025
Ca	1.815	1.610	0.431	0.226	1.929	2.335	0.216	1.861	1.531	0.830	0.128
Na	0.003	0.505	0.560	0.246	0.012	1.739	0.309	0.002	0.617	0.013	0.243
K	0.008	0.151	0.013	0.145	0.006	0.167	0.122	0.005	0.174	0.011	0.173
H	1.000	2.000	—	—	1.000	2.000	—	1.000	2.000	—	—

Note: Epidotes are normalized to 12 O atoms, 1 OH group; amphiboles are normalized to 23 O atoms, Fe<sup>3+</sup>/Fe<sub>tot</sub> = 0.2, melt compositions to 8 O atoms, all Fe as Fe<sup>2+</sup>.

rims around almandine seeds. At higher temperatures, these rims grew larger, and idiomorphic, isometric, homogeneous garnet grains up to 15 μm appear with compositions of approximately Alm<sub>50</sub>Py<sub>20</sub>Gr<sub>30</sub>. Potassium feldspar is present in few experiments close to the solidus (see also Schmidt 1992); it melts completely 10–20 °C above the wet solidus.

Melt was present in most experiments. At low melt percentages (estimated to <25 vol%), melt formed pools. At higher amounts, melt was distributed homogeneously. Round holes (bubbles) were always present in the melt, suggesting the presence of an excess fluid phase (Figs. 1A and 1B). Bubbles were always equally distributed over the entire capsule. Sometimes they carried silicate phases that obviously precipitated from the fluid, indicating that the reacted fluid was not pure H<sub>2</sub>O. Opaque phases were essentially absent in experiments where epidote is stable. However, a considerable amount of nearly Ti-free magnetite with triangular and rectangular grain shapes appeared in low-pressure experiments in which epidote was not present. Apatite was present in most experiments, characteristically exhibiting high F contents [F/(F + OH) from 0.5 to 0.8]. Other accessories included titanite, rutile, and zircon.

#### EPIDOTE MELTING REACTIONS WITH EXCESS H<sub>2</sub>O IN CALC-ALKALINE ROCK COMPOSITIONS

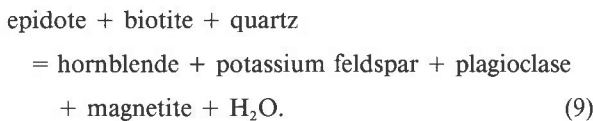
The wet (H<sub>2</sub>O-saturated) solidus of tonalite was experimentally determined by Piwinski (1–3 kbar, 1968), by Lambert and Wyllie (10–30 kbar, 1974), and slightly

modified by Schmidt (1993). The wet liquidus was determined by Egger (0.5–6.3 kbar, 1972) and by Allen and Boettcher (10–25 kbar, 1983). Figure 2 is constructed from these results and the experiments conducted for this study. Most of the reported experiments on tonalite and andesite are generally consistent, however, because similar but not identical bulk compositions were investigated, small differences are to be expected. In addition, many of the earlier experiments had problems with Fe loss to the capsule and did not control *f*<sub>O<sub>2</sub></sub> (see discussion in Allen and Boettcher 1983 and Lambert and Wyllie 1974), and this resulted in large uncertainties on the relations of Fe-Mg phases. Experiments on granodiorites are rare. Piwinski (1–3 kbar, 1968) and Piwinski (1–10 kbar, 1973) determined the solidus of natural amphibole-bearing and amphibole-free granodiorites to be about 20 °C lower than for a tonalite. Naney (2 and 8 kbar, 1983) also found a solidus 20 °C lower for a synthetic granodiorite.

#### Tonalite

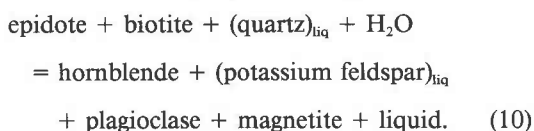
The low-pressure stability limit for magmatic epidote is defined as the intersection of the supersolidus epidote-crystallizing reaction with the solidus. However, the solidus reaction, which involves a multicomponent system, extends over a temperature interval of 10–20 °C, i.e., from the solidus to the potassium feldspar-out reaction. Thus, the subsolidus epidote-forming Reaction 9 also extends 10–20 °C above the solidus until potassium feldspar disappears. Strictly, it is at the intersection of the supersolidus epidote-forming reaction with the potassi-

um feldspar melting curve and not at the solidus where the type and slope of the epidote-out reaction changes (Fig. 2A). At water-saturated conditions,  $f_{O_2}$  buffered to NNO, magmatic epidote was present at 6 kbar (665 °C) but was absent at 4.5 kbar (680 °C). The slope of the magmatic epidote-forming reaction is relatively steep in  $P$ - $T$  space (Fig. 2A), thus its intersection with the potassium feldspar melting reaction is inferred to be  $\sim 5.5$  kbar (680 °C). The wet solidus for tonalite intersects a subsolidus epidote-dehydration reaction near 5 kbar, 660 °C. Mass-balance calculations (Reaction 1, Schmidt 1993), with mineral compositions obtained in close vicinity of the  $H_2O$ -saturated solidus, suggest that the subsolidus epidote-dehydration reaction appropriate to tonalite bulk compositions is



The left side of the reaction corresponds to the higher pressure and lower temperature side (see also Fig. 3). With increasing temperature, epidote + biotite + quartz undergo dehydration to amphibole + potassium feldspar + plagioclase +  $H_2O$ ; the Clapeyron slope of this reaction was calculated to approximately 40 °C/kbar (Schmidt 1993). The role of magnetite in this reaction is difficult to assess by mass-balance calculations because magnetite appeared only in minor amounts. However, as concluded from reported experiments (Schmidt 1993) and as indicated by field evidence (Hammarstrom and Zen 1992, personal communication), magnetite is significantly more abundant in epidote-free than in epidote-bearing granitoid intrusions. Such an observation was also reported by Drinkwater et al. (1991) for the coast plutonic-metamorphic complex near Juneau, Alaska. This indicates that, at low pressures, magnetite is the principal phase containing  $Fe^{3+}$  at temperatures above epidote stability. In the pressure range from 5 to 9 kbar, melting reactions involving phases similar to those in Reaction 9 occur at temperatures above the  $H_2O$ -saturated tonalite solidus.

In experimental studies on multicomponent systems representative of real rock compositions, it is not easy to separate discontinuous reactions that distinguish  $P$ - $T$  facies in the multisystem from continuous reactions appropriate for a specific bulk composition. Thus, our experimental results suggest that the pertinent multisystem discontinuous reaction delimiting epidote stability in tonalite melts with excess  $H_2O$  (see also Fig. 3) is



Quartzofeldspathic components are written in parentheses because at  $H_2O$ -saturated conditions these minerals sequentially melt at temperatures not much higher than the  $H_2O$ -saturated solidus. Potassium feldspar and quartz

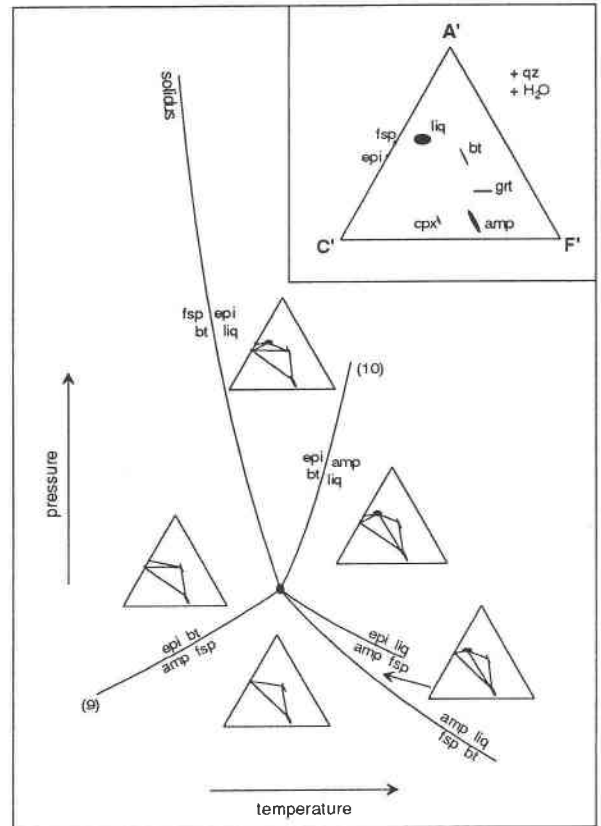
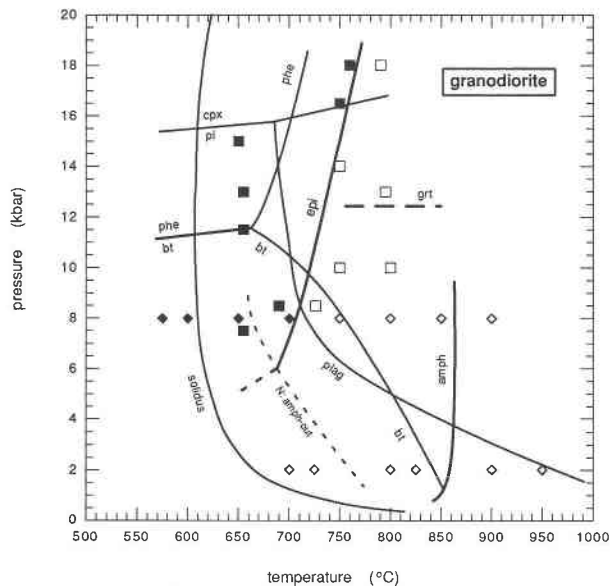


FIGURE 3. Topology of epidote melting and crystallization reactions in tonalite- $H_2O$ -NNO near the solidus. The invariant point is located near 5 kbar, 680 °C. The phase relations are portrayed with an "ACF-de-luxe" projection from quartz and  $H_2O$ . Because this projection condenses along the vectors  $Na-SiCa_{-1}Al_{-1}$ ,  $NaK_{-1}$ ,  $Fe^{2+}Mg_{-1}$ , and  $Fe^{3+}Al_{-1}$  (Thompson 1982, p. 27), some details of the reaction topologies involving these exchange vectors cannot be illustrated simply. In the natural samples, the solidus reaction in the ACF diagram is split into a potassium feldspar-quartz (qz)-biotite (bt)-plagioclase (plag)- $H_2O$  and a qz-bt-plag- $H_2O$  reaction, which spread over approximately 50 °C. Feldspar is indicated by fsp.

melt at temperatures approximately 10–20 and 30–50 °C above the water-saturated solidus, respectively (Fig. 2A). Reaction 10 delimits the epidote + biotite stability field in the pressure interval from 5 to 9 kbar. It is possible to write subsets of the epidote + biotite melting Reaction 10 as continuous equilibria appropriate to the sequential melting of potassium feldspar and quartz. Such mass-balanced continuous reactions (written with respect to quartzofeldspathic melt components) are only appropriate to the bulk compositions considered.

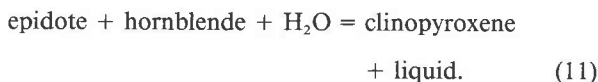
More difficult to ascertain is the nature of the multisystem epidote-melting reactions between the disappearance of biotite ( $\sim 9$  kbar, 720 °C) and plagioclase ( $\sim 10$  kbar, 740 °C) and the appearance of clinopyroxene ( $\sim 11$  kbar, 770 °C). In fact, discontinuous Reaction 10 removes biotite from the tonalite bulk composition such



**FIGURE 4.** Pressure-temperature diagram for granodiorite melting at water-saturated conditions with  $f_{O_2}$  buffered by NNO. The  $H_2O$ -saturated solidus is from Naney (1983) and Piwinski (1968). The reaction boundaries are interpolated between the 2 and 8 kbar experiments of Naney (1983; diamonds) and the present study (squares, Table 2). Solid symbols contain epidote, open do not. Garnet appears near 13 kbar in high-temperature experiments. Experiments close to the solidus did not have garnet seeds and failed to nucleate garnet; thus, these experiments are not suitable for delineation of the garnet-in reaction near the solidus. The maximal melting temperature of epidote in granodiorite- $H_2O$  is about 30 °C lower than in tonalite- $H_2O$ . The biotite-out reaction intersects the plagioclase-out reaction (plag) twice (near 5 and 10 kbar). On the basis of Naney's (1983) experiments, amphibole only appears some 50 °C above the granodiorite solidus (dashed line N). This results in a subsolidus dehydration reaction for epidote without amphibole.

that it would only appear in more mafic ("gabbroic") compositions (Fig. 3). The continuous reaction involving biotite + amphibole + melt is fundamental in calc-alkaline magma fractionation (Abbott 1982; Speer 1987).

The clinopyroxene-in reaction in tonalite- $H_2O$  melts intersects the epidote-melting reaction near 11 kbar, 770 °C. Melting of epidote above the clinopyroxene-in reaction is directly related to the appearance of clinopyroxene, that is, with increasing temperature modal increase in clinopyroxene is directly proportional to epidote decrease. Our experimental results can be represented by the multisystem discontinuous reaction



Thus, at pressures along the epidote melting curve for  $H_2O$ -saturated tonalite melts, amphibole changes from a high-temperature reactant (Reaction 10) to a lower temperature product when clinopyroxene appears. A similar

peritectic melting reaction occurs in the model system CMASH (Thompson and Ellis 1994).

In water-saturated tonalite, garnet is formed at relatively high pressures through a series of different reactions from 600 to 950 °C at pressures ranging from 14 to 16 kbar. The maximum temperature stability of 790 °C of magmatic epidote in tonalite is reached near 14 kbar, i.e., at the intersection with the mostly pressure-dependent garnet-in reaction. This maximum temperature results from the change in Clapeyron slopes ( $dP/dT$ ) of the epidote-melting reactions from positive at low pressures to negative at high pressures in the presence of garnet + clinopyroxene (Fig. 2A).

### Granodiorite

Experiments were performed with granodiorite (Au7) at pressures from 7 to 18 kbar and  $H_2O$  saturation, with  $f_{O_2}$  controlled by NNO (Fig. 4). In the range from 7 to 10 kbar, where the granodiorite assemblage hornblende + plagioclase + biotite is the same as in the tonalite, the locations of the epidote-melting reactions are almost identical (Fig. 2B). In this pressure range, a reaction similar to that in the tonalite (Reaction 10) is probably appropriate for the granodiorite. Toward high pressures (~10–15 kbar), the stability limit of epidote is about 30 °C lower in the granodiorite than in the tonalite (Fig. 2B). However, the experimental data are not sufficient to determine the epidote-melting reactions in granodiorite at high pressures. In contrast to tonalite, clinopyroxene does not appear until 18 kbar. Garnet growth rims form at pressures >13 kbar in experiments that contained garnet seeds (Table 1). At 18 kbar, granodiorite Au7 contains the same assemblage as tonalite RPR: hornblende + garnet + clinopyroxene ± epidote. Thus, it is expected that at ~18 kbar the epidote-melting reaction in the granodiorite would also have a negative slope in  $P$ - $T$  space.

At low temperatures, the experiments of Naney (1983) on a synthetic granodiorite composition indicate that hornblende is not stable below approximately 680 °C (dashed line marked "N" in Fig. 4). This implies that at low temperatures there are fundamental differences in the  $H_2O$ -saturated melting reactions occurring in granodiorite and tonalite compositions. In tonalite, amphibole forms part of the subsolidus assemblage, whereas in Naney's granodiorite, amphibole was generated only above the solidus (both at 2 and 8 kbar) by reactions involving biotite + feldspar + quartz. The experiments by Piwinski (1968), however, showed amphibole to be stable down to subsolidus temperatures in several granodiorite compositions. Because of the paucity of experiments near the  $H_2O$ -saturated granodiorite solidus between 2 and 8 kbar, it is not yet possible to identify the precise epidote-melting reaction in granodiorite in this pressure range.

### MAGMATIC EPIDOTE AS AN INDICATOR OF MINIMUM INTRUSION PRESSURE AND THE INFLUENCE OF $f_{O_2}$

Epidote crystallizes from tonalitic or granodioritic magmas only above a certain pressure (Zen and Ham-

marstrom 1984), thus the very presence of epidote in such a magma body is suitable to define a minimum intrusion pressure. Because epidote exhibits  $\text{Fe}^{3+}\text{Al}_{-1}$  exchange, its stability also depends upon  $f_{\text{O}_2}$ . The experiments in the synthetic CFASH system by Holdaway (1972) and Liou (1973) demonstrated that the  $P$ - $T$  location and stoichiometry of subsolidus-epidote dehydration reactions, as well as epidote composition, strongly depend on  $f_{\text{O}_2}$ . For an  $f_{\text{O}_2}$  buffered from NNO to HM, the epidote stability field in the synthetic system is extended about 2 kbar toward lower pressures. Because these dehydration reactions have positive  $dP/dT$ , epidote stability is also displaced toward higher temperatures. Similar behavior is observed in our melting experiments on natural tonalite (Fig. 5). At an  $f_{\text{O}_2}$  buffered at NNO, epidote is stable at temperatures above the water-saturated solidus at pressures  $> 5$  kbar (Figs. 2A and 5). Although most experiments were conducted with  $f_{\text{O}_2}$  buffered by NNO, several experiments were conducted at an  $f_{\text{O}_2}$  buffered by HM (Table 1, Fig. 5). At these fairly oxidizing conditions, the magmatic stability of epidote is extended toward lower pressures and higher temperatures. The intersection of the subsolidus-epidote dehydration reaction at  $f_{\text{O}_2} = \text{HM}$  with the  $\text{H}_2\text{O}$ -saturated tonalite solidus is located at a pressure of about 3 kbar (Fig. 5). By applying the Al-in-hornblende geobarometer to epidote-bearing granitoids, Vyhnaal et al. (1991) concluded that a minimum pressure of  $\sim 2.8$  kbar (using the calibration of Schmidt 1992) is required for epidote formation.

As can be seen in Figure 5, both epidote-melting reactions in the tonalite at  $f_{\text{O}_2} = \text{NNO}$  and  $f_{\text{O}_2} = \text{HM}$ , with excess  $\text{H}_2\text{O}$ , lie close to extrapolated subsolidus-epidote dehydration reactions in the synthetic CFASH-system at equivalent oxygen fugacities (as determined by Holdaway 1972 and Liou 1973).

Intermediate (calc-alkaline) granitoid magmas mostly crystallize quartz, magnetite, and titanite. Quartz + magnetite define the lower limit of  $f_{\text{O}_2}$  close to the quartz + fayalite + magnetite (QFM) buffer. An upper limit of oxidation is provided by the presence of ilmenite in many intermediate granitoids (Ishihara 1977, 1981; Murata and Itaya 1987; Hammarstrom and Zen 1992), which defines an  $f_{\text{O}_2}$  lower than the magnetite + ilmenite + rutile buffer (MIR). Wones (1989) showed that the assemblage quartz + magnetite + titanite requires  $f_{\text{O}_2}$  slightly above QFM. Thus, for most granitoid intrusions, the intrinsic oxidation conditions are experimentally most usefully reproduced by the NNO buffer, and the results from these experiments are therefore directly applicable to most natural tonalite intrusions. However, because more oxidizing conditions might occur in some plutons (documented by iron titanium oxides, or in extreme cases by the presence of hematite, e.g., Ishihara 1981) and because epidote crystallization conditions are favored by more oxidized magmas, the use of epidote reactions as geobarometers is applicable only if the  $f_{\text{O}_2}$  of the magma can be determined. Although  $f_{\text{O}_2}$  conditions are not likely to fluctuate wildly during magma crystallization, the  $f_{\text{O}_2}$  may step from

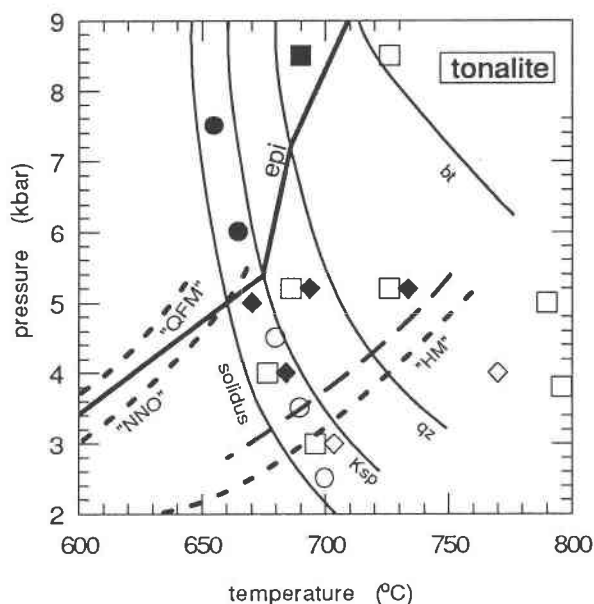


**FIGURE 5.** Pressure-temperature diagram showing the stability of epidote in tonalite- $\text{H}_2\text{O}$  with  $f_{\text{O}_2}$  buffered by NNO (squares and circles) and HM (diamonds). Solid lines are phase boundaries at  $f_{\text{O}_2} = \text{NNO}$ , the long-dashed line represents the approximate location of the epidote-out reaction at  $f_{\text{O}_2} = \text{HM}$ . Solid symbols for experiments containing epidote. Increasing  $f_{\text{O}_2}$  from NNO to HM increases the thermal stability of epidote in tonalite melts and moves the intersections with the phase disappearance curves to lower pressure. "QFM," "NNO," and "HM" label epidote-delimiting reactions at their respective  $f_{\text{O}_2}$  buffers from Liou (1973). Both the NNO and HM epidote-forming reactions of the synthetic CFASH system of Liou (1973) are very close to the epidote-out reactions in the tonalite.

buffer to buffer as particular  $\text{Fe}^{3+}$ -bearing minerals are replaced by others (magnetite by epidote, or in some cases by acmite or riebeckite) or when the fluid composition changes drastically (physically by phase separation, or chemically through C-O-H-S reactions). This latter effect is likely to happen at the borders of intrusions where interaction with the surrounding country rock is facilitated.

A more subtle effect of  $f_{\text{O}_2}$  variation involves the rare-earth enriched allanite. Allanite commonly occurs as cores in magmatic epidote (Zen and Hammarstrom 1984; Moench 1986; Tulloch 1986; Evans and Vance 1987; Zen 1988) and is presumably stable to higher temperatures than common epidote.

## DISCUSSION

The greatest pressure recorded by the Al-in-hornblende geobarometer in epidote-bearing calc-alkaline intrusions is about 8 kbar (Hammarstrom and Zen 1986). This pressure corresponds to a depth of about 28 km, which is within continental crust of normal thickness. The present results for melting reactions for tonalite and granodiorite

**TABLE 4.** Examples of modal abundances

Expt.	r47	r65	r76
<i>P</i> (kbar)	10	13	18
<i>T</i> (°C)	725	775	760
epi	4.1	1.4	5.4
amph	24.1	28.1	22.3
plag	2.5	—	—
gar	—	—	7.6
liq	69.3	70.5	64.7

Note: Modal abundances are given in oxygen percent, which are similar to the volume percent values. For method of calculation see Schmidt (1993). Errors are on the order of 5–10% of each value.

are directly applicable to calc-alkaline magma crystallization at H<sub>2</sub>O saturation at any depth in continental crust.

### Epidote crystallization in tonalite

The minimum pressure required for the appearance of epidote in calc-alkaline intrusions could vary because of potential differences in  $f_{O_2}$  during tonalite crystallization (Fig. 5) and because of compositional changes from tonalite toward more granodioritic compositions (compare Figs. 2 and 4). The present experiments on epidote stability in H<sub>2</sub>O-saturated tonalite composition reveal that the first appearance of epidote during the crystallization history of a cooling magma could provide a more detailed geobarometer. At H<sub>2</sub>O saturation and pressures to about 11 kbar (Fig. 2) the sequence of crystallization in tonalite is hornblende → plagioclase → biotite → quartz → potassium feldspar. The position of epidote moves from left to right in this sequence as pressure decreases. At pressures higher than 10 kbar epidote appears between hornblende and plagioclase, from 10 to 8 kbar epidote appears between plagioclase and biotite, from 8 to 6 kbar epidote appears between biotite and quartz, and between 6 and 5 kbar epidote appears between quartz and potassium feldspar. All these various crystallization sequences for epidote have been reported in the literature (for example, the references cited by Tulloch, Moench, and Zen and Hammarstrom in their exchange of correspondence in 1986). The pressures listed here apply to the experiments with  $f_{O_2}$  buffered by NNO and at H<sub>2</sub>O saturation. Although the actual pressures of epidote crystallization would be lowered with  $f_{O_2}$  buffered at a higher value (e.g., HM), the order of epidote in the crystallization sequences is likely to persist.

Our experimental results have application to a few other petrographic observations. The epidote-melting reactions in the range 5–9 kbar for tonalite + H<sub>2</sub>O ( $f_{O_2}$  = NNO) may also be considered, in reverse, as the crystallization of epidote + biotite simultaneous with peritectic resorption of some hornblende by the melt. This interpretation is in accordance with observed crystallization textures in tonalites (e.g., Cornelius 1915; Hammarstrom and Zen 1986). However, as can be seen from Figures 2A and 3, at pressures <9 kbar, biotite begins to crystallize before epidote. Hornblende is consumed by reaction with

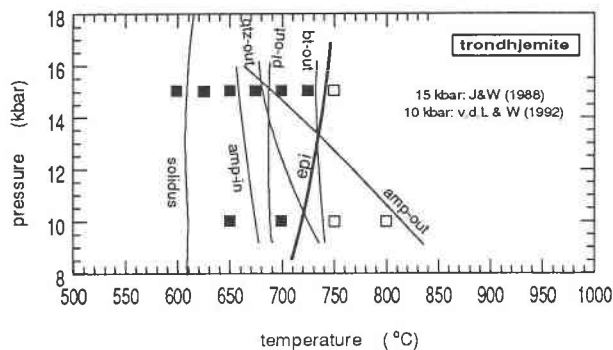


**FIGURE 6.** Pressure-temperature diagram for trondhjemite at H<sub>2</sub>O-saturated conditions,  $f_{O_2}$  unbuffered. Compiled from Johnston and Wyllie (1988) and van der Laan and Wyllie (1992).

the melt (Eq. 10), and its modal decrease should be mirrored by proportional increase in modes of epidote and biotite. Consequently, the local resorption of hornblende through the appearance of epidote and the growth of biotite does not imply a general destabilization of hornblende in the tonalite melt (Fig. 3) but a decrease in modal abundance.

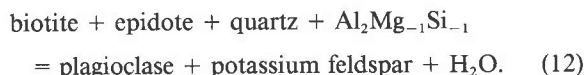
Modal abundances of epidote were calculated from phase compositions employing a mass-balance program (NTCARLO, for description see Schmidt 1993). Modal abundances of epidote are generally low near the epidote-out reactions (1–5 vol%, Table 4) but increase to 11–14 vol% near the solidus (Fig. 12, Schmidt 1993). The amount of liquid is on the order of 60–70 vol% when epidote starts to crystallize. Thus, fractionation of epidote is possible at water-saturated conditions; however, epidote contents are low, and a significant effect of epidote fractionation on bulk composition appears to be unlikely. By contrast, fractionation of LREE-enriched epidote or allanite may modify the trace element patterns in specific cases.

Our experimental results are consistent with suggestions that epidote inclusions in biotite (e.g., in high-level oxidized granitoids, Tulloch 1986) and epidote grains that crystallized when the melt proportion was 50–80% (as in the rhyodacite dykes described by Evans and Vance 1987) are xenocrysts carried from depth. In the pressure range from 10 to 15 kbar in tonalite + H<sub>2</sub>O ( $f_{O_2}$  = NNO, Fig. 2A) and in granodiorite + H<sub>2</sub>O ( $f_{O_2}$  = NNO, Fig. 4), epidote crystallizes before biotite. However, it is not likely that H<sub>2</sub>O-saturation is reached in the early stages of magmatic crystallization, so the question arises about the crystallization sequences at water contents appropriate for the H<sub>2</sub>O-undersaturated region.

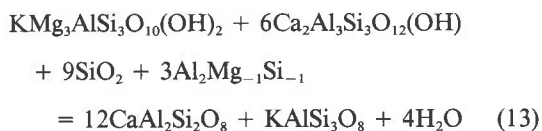
### Crystallization of mafic minerals in tonalite-trondhjemite-granodiorite compositions

The epidote-melting reactions are located at similar *P-T* conditions in H<sub>2</sub>O-saturated experiments on tonalite, granodiorite, and trondhjemite (Figs. 2B and 6). At pressures lower than approximately 8 kbar, the nature of the

epidote-out reaction depends on the stability of amphibole in the various rock compositions. For example, in trondhjemite (Johnston and Wyllie 1988; van der Laan and Wyllie 1992) and in granodiorite (Naney 1983) amphibole is not stable at the H<sub>2</sub>O-saturated solidus. In contrast, Piwinski's (1968) experiments on granodiorite suggest that amphibole is stable at the H<sub>2</sub>O-saturated solidus. In the presence of amphibole, the epidote-out reactions in granodiorite are similar to that discussed above for tonalite (Reaction 10). In the absence of amphibole, the likely reaction for the disappearance of epidote in granodiorite and trondhjemite, which continues into the subsolidus region, is the amphibole-absent continuous reaction



When written for KCMASH components, this continuous reaction has the coefficients



and forms plagioclase from epidote by consuming Al<sub>2</sub>Mg<sub>-1</sub>Si<sub>-1</sub> (Tschermak-exchange) in biotite.

In any particular multisystem (e.g., KCMASH as in Reaction 12), this amphibole-absent continuous reaction in granodiorite occurs at higher pressures and lower temperatures than the discontinuous Reaction 10 in tonalite. Field evidence indicates that at pressures up to 7 kbar, epidote is less stable in granodiorite than in tonalite because in many intrusions epidote-bearing tonalite is found adjacent to epidote-free granodiorite (e.g., Bregaglia, Moticska 1970).

Estimation of the behavior of epidote at water-undersaturated conditions remains difficult. The experimental results of van der Laan and Wyllie (1992) and Johnston and Wyllie (1988) at 10 and 15 kbar for trondhjemite indicate an increase in epidote stability of 10 to 25 °C with decreasing water content in the melting region, whereas experiments by Naney (1983) at 8 kbar on granodiorite indicate a decrease in epidote stability of about 20 °C with decreasing water content. Experiments at pressures above 8 kbar on a hornblende-bearing dacite at 3 and 5% water content (Green 1992) did not produce epidote, 800 °C being the lowest temperature investigated. This indicates that in granodiorite (at 15 kbar) the epidote stability field does not substantially enlarge with decreasing water content. Experiments on an epidote-bearing tonalite with no water added (Skjerlie and Johnston 1993) did not result in stable epidote, the lowest temperature investigated being 875 °C at 10 kbar. Further comments on epidote stability in the H<sub>2</sub>O-undersaturated region cannot be made without additional experiments. Unfortunately, it is a formidable experimental task to vary systematically *f*<sub>O<sub>2</sub></sub>, bulk rock composition, and H<sub>2</sub>O content

as functions of pressure and temperature, especially because the conventional solid-phase *f*<sub>O<sub>2</sub></sub> buffers require an excess of H<sub>2</sub>O to operate. Additional field observations using some of our experimental results could help to constrain some of the many variables in the crystallization of calc-alkaline plutons.

### CONCLUDING REMARKS

These experimental results on epidote stability in calc-alkaline magmas contribute to the tools we have available to evaluate the evolution of physical parameters during the cooling of the most abundant types of batholiths. Simultaneous consideration of the various assemblages enables determination of *P* (depth), *T*, *f*<sub>H<sub>2</sub>O</sub>, *f*<sub>O<sub>2</sub></sub>, and their interrelationships during magmatic cooling. For example, the procedures used by Evans and Vance (1987) illustrate the dependence of *T*, *f*<sub>H<sub>2</sub>O</sub>, and *f*<sub>O<sub>2</sub></sub> in a natural magmatic assemblage.

The original empirical calibration of the Al-in-hornblende barometer (Hammarstrom and Zen 1986) was made using geobarometric pressure estimates from assemblages in the surrounding contact aureoles (see confirmation by Hollister et al. 1987). The very success of the Al-in-hornblende geobarometer indicates that whatever their depth of origin, calc-alkaline intrusions equilibrate at their depths of final emplacement. Divergence of intrusive pressures determined by use of the experimentally calibrated Al-in-hornblende (Schmidt 1992) from values of pressure given by aureole assemblages can be specifically related to *a*<sub>H<sub>2</sub>O</sub> in the magma [see Schmidt's appraisal of Johnson and Rutherford's (1989) experiments conducted for *x*<sub>H<sub>2</sub>O</sub> = 0.5]. Thus, with the ranges of the physical parameters determined, the position of epidote in the crystallization sequence (Figs. 2 and 4 here) and the consideration of the mineral textures can be used to obtain the changing proportions of minerals to magma as well as the variations of *a*<sub>H<sub>2</sub>O</sub> and *f*<sub>O<sub>2</sub></sub> in the magma during the cooling history. It is important to obtain these because there have been no determinations of melt-crystal fraction since the H<sub>2</sub>O-saturated experiments by Piwinski (1968, 1973) on tonalite-granodiorite melts.

### ACKNOWLEDGMENTS

These experiments were conducted from 1989 to 1993 in the laboratories at IMP, Eidgenössische Technische Hochschule, Zurich; at "Depths of the Earth," Arizona State University (ASU), Tempe; and at URA-10, Clermont-Ferrand. To all our colleagues in these labs, especially Daniel Vielzeuf and John Holloway, we owe our thanks for help and collaboration. We thank W. Oberholzer, E. Reusser, and P. Ulmer for supplying starting materials. The stay of M.W.S. at ASU was financed through a scholarship from Eidgenössische Technische Hochschule, Zurich, and the visit at Clermont-Ferrand was supported through a postdoctoral fellowship from the Suisse National Fond.

### REFERENCES CITED

- Abbott, R.N., Jr. (1982) A petrogenetic grid for medium and high grade metabasites. *American Mineralogist*, 67, 865-876.  
 Allen, J.C., and Boettcher, A.L. (1983) The stability of amphibole in andesite and basalt at high pressures. *American Mineralogist*, 68, 307-314.

- Apted, M.J., and Liou, J.G. (1983) Phase relations among greenschist, epidote-amphibolite, and amphibolite in a basaltic system. *American Journal of Science*, 283A, 328–354.
- Boettcher, A.L. (1970) The system  $\text{CaO-Al}_2\text{O}_3\text{-SiO}_2\text{-H}_2\text{O}$  at high pressures and temperatures. *Journal of Petrology*, 11, 337–379.
- Cornelius, H.P. (1915) Geologische Beobachtungen im Gebiet des Forno-Gletschers (Engadin). *Centralblatt für Mineralogie Geologie und Paläontologie* 1913, 8, 246–252.
- Crawford, M.L., and Hollister, L.S. (1982) Contrast of metamorphic and structural histories across the Work Channel lineament, Coast Plutonic Complex, British Columbia. *Journal of Geophysical Research*, 87, 3849–3860.
- Drinkwater, J.L., Ford, A.B., and Brew, D.A. (1991) Magnetic susceptibilities and iron content of plutonic rocks across the Coast Plutonic-Metamorphic Complex near Juneau, Alaska. In D.C. Bradley and C. Dusel-Bacon, Eds., *Geologic studies in Alaska by the U.S. Geological Survey*, U.S. Geological Survey Bulletin 2041, 125–139.
- Eggler, D.H. (1972) Water-saturated and undersaturated melting relations in a Paricutin andesite and an estimate of water content in the natural magma. *Contributions to Mineralogy and Petrology*, 34, 261–271.
- Ellis, D.J., and Thompson, A.B. (1986) Subsolidus and partial melting reactions in the quartz-excess  $\text{CaO} + \text{MgO} + \text{Al}_2\text{O}_3 + \text{SiO}_2 + \text{H}_2\text{O}$  system under water-excess and water-deficient conditions to 10 kb: Some implications for the origin of peraluminous melts from mafic rocks. *Journal of Petrology*, 27, 91–121.
- Evans, B.W., and Vance, J.A. (1987) Epidote phenocrysts in dacitic dikes, Boulder County, Colorado. *Contributions to Mineralogy and Petrology*, 96, 178–185.
- Green, T.H. (1992) Experimental phase equilibrium studies of garnet-bearing I-type volcanics and high level intrusives from Northland, New Zealand. *Transactions of the Royal Society of Edinburgh: Earth Sciences*, 83, 429–438.
- Hammarstrom, J.M., and Zen, E-an (1986) Aluminum in hornblende: An empirical igneous geobarometer. *American Mineralogist*, 71, 1297–1313.
- (1992) Petrological characteristics of magmatic epidote-bearing granites of the western cordillera of America (abs.). *Transactions of the Royal Society of Edinburgh: Earth Sciences*, 83, 490–491.
- Holdaway, M.J. (1972) Thermal stability of Al-Fe-epidote as a function of  $f_{\text{O}_2}$  and Fe content. *Contributions to Mineralogy and Petrology*, 37, 307–340.
- Hollister, L.S., Grissom, G.C., Peters, E.K., Stowell, H.H., and Sisson, V.B. (1987) Confirmation of the empirical correlation of Al in hornblende with pressure of solidification of calc-alkaline plutons. *American Mineralogist*, 72, 231–239.
- Ishihara, S. (1977) The magnetite-series and ilmenite-series granitic rocks. *Mining Geology*, 27, 293–305.
- (1981) The granitoid series and mineralization. *Economic Geology*, 75th anniversary volume, 458–484.
- Johnson, M.C., and Rutherford, M.J. (1989) Experimental calibration of the aluminum-in-hornblende geobarometer with application to Long Valley caldera (California) volcanic rocks. *Geology*, 17, 837–841.
- Johnston, A.D., and Wyllie, P.J. (1988) Constraints on the origin of Archean trondhjemites based on phase relationship of Nük gneiss with  $\text{H}_2\text{O}$  at 15 kbar. *Contributions to Mineralogy and Petrology*, 100, 35–46.
- Kress, V.C., and Carmichael, I.S.E. (1988) Stoichiometry of the iron oxidation reaction in silicate melts. *American Mineralogist*, 73, 1267–1274.
- Lambert, I.B., and Wyllie, P.J. (1974) Melting of tonalite and crystallization of andesite liquid with excess water to 30 kilobars. *Journal of Geology*, 82, 88–97.
- Liou, J.G. (1973) Synthesis and stability relations of epidote,  $\text{Ca}_2\text{Al}_2\text{FeSi}_3\text{O}_{12}(\text{OH})$ . *Journal of Petrology*, 14, 381–413.
- Moench, R.H. (1986) Comment on "Implications of magmatic epidote-bearing plutons on crustal evolution in the accreted terranes of northwestern North America" and "Magmatic epidote and its petrologic significance." *Geology*, 14, 187–188.
- Motievska, P. (1970) Petrographie und Strukturanalyse des westlichen Bergeller Massivs und seines Rahmens. *Schweizerische Mineralogische und Petrographische Mitteilungen*, 50, 355–443.
- Murata, M., and Itaya, T. (1987) Sulfide and oxide minerals from S-type and I-type granitic rocks. *Geochimica et Cosmochimica Acta*, 51, 497–507.
- Naney, M.T. (1983) Phase equilibria of rock-forming ferromagnesian silicates in granitic systems. *American Journal of Science*, 283, 993–1033.
- Newton, R.C. (1966) Some calc-silicate equilibrium relations. *American Journal of Science*, 264, 204–222.
- Nitsch, K.H., and Winkler, H.G.F. (1965) Bildungsbedingungen von Epidot und Orthozoisit. *Beiträge zur Mineralogie und Petrographie*, 11, 470–486.
- Piwinskii, A.J. (1968) Experimental studies of igneous rock series: Central Sierra Nevada batholith, California. *Journal of Geology*, 76, 548–570.
- (1973) Experimental studies of igneous rock series, central Sierra Nevada batholith, California: Part II. *Neues Jahrbuch für Mineralogie*, 5, 193–215.
- Pouchon, J.L., and Pichoir, F. (1984) Un nouveau modèle de calcul pour la microanalyse quantitative par spectrométrie de rayon X: Partie I. Application à l'analyse d'échantillons homogènes. *La Recherche Aérospatiale*, 3, 167–192.
- Schmidt, M.W. (1992) Amphibole composition in tonalite as a function of pressure: An experimental calibration of the Al-in-hornblende-barometer. *Contributions to Mineralogy and Petrology*, 110, 304–310.
- (1993) Phase relations and compositions in tonalite as a function of pressure: An experimental study at 650 °C. *American Journal of Science*, 293, 1011–1060.
- Skjerlie, K.P., and Johnston, A.D. (1993) Fluid-absent melting behavior of an F-rich tonalitic gneiss at mid-crustal pressures: Implications for the generation of anorogenic granites. *Journal of Petrology*, 34, 785–815.
- Speer, J.A. (1987) Evolution of magmatic AFM mineral assemblages in granitoid rocks: The hornblende + melt = biotite reaction in the Liberty Hill pluton, South Carolina. *American Mineralogist*, 72, 863–878.
- Strens, R.G.J. (1965) Stability and relations of the Al-Fe epidotes. *Mineralogical Magazine*, 35, 464–475.
- Thompson, A.B., and Ellis, D.J. (1994)  $\text{CaO} + \text{MgO} + \text{Al}_2\text{O}_3 + \text{SiO}_2 + \text{H}_2\text{O}$  to 35 kbar: Amphibole, talc and zoisite dehydration and melting reactions in the silica-excess part of the system and their possible significance in subduction zones, amphibolite melting and magma fractionation. *American Journal of Science*, 294, 1229–1289.
- Thompson, J.B. (1982) Composition space: An algebraic and geometric approach. In *Mineralogical Society of America Reviews in Mineralogy*, 10, 1–32.
- Tulloch, A.J. (1986) Comment on "Implications of magmatic epidote-bearing plutons on crustal evolution in the accreted terranes of northwestern North America" and "Magmatic epidote and its petrologic significance." *Geology*, 14, 187–188.
- van der Laan, S.R., and Wyllie, P.J. (1992) Constraints on Archean trondhjemite genesis from hydrous crystallization experiments on Nük Gneiss at 10–17 kbar. *Journal of Geology*, 100, 57–68.
- Vyhnal, C.R., McSween, H.Y., Jr., and Speer, J.A. (1991) Hornblende chemistry in southern Appalachian granitoids: Implications for aluminum hornblende thermobarometry and magmatic epidote stability. *American Mineralogist*, 76, 176–188.
- Wones, D.R. (1989) Significance of the assemblage titanite + magnetite + quartz in granitic rocks. *American Mineralogist*, 74, 744–749.
- Zen, E-an (1988) Tectonic significance of high-pressure plutonic rocks in the western cordillera of North America. In *Metamorphism and Crustal Evolution of the Western United States*, Rubey volume VII, 41–67.
- Zen, E-an, and Hammarstrom, J.M. (1984) Magmatic epidote and its petrologic significance. *Geology*, 12, 515–518.
- (1986) Reply on the comments on "Implications of magmatic epidote-bearing plutons on crustal evolution in the accreted terranes of northwestern North America" and "Magmatic epidote and its petrologic significance" by A.J. Tulloch and by R.H. Moench. *Geology*, 14, 187–188.